SUPPLEMENTARY METHODS

Patient sample processing, cell lines, and cell culture

Human peripheral blood mononuclear cells were isolated from CLL patients or healthy donors using Ficoll density gradient centrifugation (Ficoll-Plaque Plus; Amersham Biosciences Inc, Piscataway, NJ). Enriched B cell fractions were prepared using the RosetteSep™ B-cell kit (STEMCELL Technologies, Vancouver Canada) according to the manufacturer's instructions. Isolated cells were incubated in RPMI 1640 media (Invitrogen, Grand Island, NY) supplemented with 10 % heat-inactivated fetal bovine serum (Sigma-Aldrich, St. Louis, MO), 2 mM L-glutamine (Invitrogen), and 100 U/mL penicillin / 100 µg/mL streptomycin (Sigma-Aldrich) at 37°C in an atmosphere of 5 % CO2. The purity of enriched populations of CLL was routinely checked using CD19-PE (BD Pharmingen, Billerica, MA) staining by flow cytometry. The CLL leukemic cell line MEC-1 was obtained from DSMZ (Braunschweig, Germany).

T-cell culture experiments

Human PBMCs were isolated from freshly donated blood from healthy donors using Ficoll density gradient centrifugation and enriched T-cell fractions were prepared using the RosetteSep™ CD3 selection kit (STEMCELL Technologies) according to the manufacturer's instructions. Isolated cells were incubated in RPMI-1640 supplemented media as described above. T-cell purity was checked using CD3-PE (BD Pharmingen) staining by flow cytometry.

For carboxyfluorescein succinimidyl ester (CFSE) labelling, T-cells were resuspended in PBS at a final concentration of $1E^7$ cells/mL and labelled with 1 µ CFSE; (Molecular Probes™, Eugene, OR) for 10 min at 37°C, 5 % CO2. The staining was quenched by adding 5 volumes of RPMI-1640 supplemented media followed by a 5-min incubation at room temperature, and excess dye was washed away. CFSE-labelled cells were cultured at a concentration of $0.5E^6$ cells/mL and to induce T-cell proliferation the cells were stimulated with plate-bound anti-CD3 and soluble anti-CD28 (eBiosciences, San Diego, CA) and treated with either DMSO (vehicle) or PLX51107. Cultures were maintained at 37°C for 4 days and were subsequently stained with anti-CD45-AF700, anti-CD4-V450, anti-CD8-BV510 (Becton Dickinson, San Jose, CA) and subjected to flow cytometric analysis on FC500 cytometer (Beckman-Coulter, Indianapolis, IN). The LIVE/DEAD Fixable near-IR stain (Invitrogen) was used to gate on viable cells and CD4 and CD8 cells were individually investigated for CFSE dilution resulting from proliferation. Data analysis was performed using Kaluza software (Beckman Coulter, Indianapolis, IN). For T-cell cultures that were maintained for 8 days, the treatment was washed out at day 4 and cells were cultured for another 4 days without treatments or with treatments (DMSO *vs.* PLX51107) for another 4 days during which cells were stimulated by placing them on anti-CD3 coated plates and adding soluble anti-CD28. Palbociclib and Fludarabine (Sigma-Aldrich) were used as control drugs to inhibit proliferation and viability, respectively.

Proliferation assay and flow cytometric studies: MTS assay was performed using the tetrazolium compound [3-(4,5-dimethylthiazol-2-yl)-5-(3-carboxymethoxyphenyl)-2-(4-sulfophenyl)-2H-tetrazolium, inner salt; MTS] and an electron coupling reagent (phenazine ethosulfate; PES) from Promega (Madison, WI). Cell apoptosis was evaluated by Annexin V-FITC or PE and propidium iodide (PI) staining using FC500 cytometer (Beckman-Coulter, Indianapolis, IN) following manufacturer's procedure (BD Pharmingen, Billerica, MA). Data analysis was performed using Kaluza software (Beckman Coulter, Indianapolis, IN). For cell cycle analysis, cells were fixed with cold ethanol overnight and then stained before analysis with 30 μg/mL propidium iodide (Invitrogen) and 200 μg/mL RNase (Sigma-Aldrich) in 0.1 % v/v Triton X-100 (Sigma-Aldrich). Cell cycle data analysis was performed using ModFit LT software (Verity Software House, Topsham, ME).

Reagents antibodies and primers

CpG685 oligonucleotide was obtained from the OSU Cytogenetics Core Lab. Antibodies used for immunoblots included anti-BRD4 (E2A7X, #13440), anti-BRD2 (D89B4, #5848), anti-cMyc (D84C12; #5605), anti-BATF (D7C5, #8638), anti-BCL6 (D65C10, #5650), anti-BTK (D3H5, #8547), anti-IKZF1/Ikaros (#5443), anti-IKZF3/Aiolos (D1C1E, #15103), anti-ZBTB17/Miz-1 (D7E8B, #14300), anti-HEXIM1 (D5Y5K, #12604) and anti-IL-2Rα/CD25 (D6K5F, #13517) from Cell Signaling Technologies (Danvers, MA); anti-BRD3 (#61489) from Active Motif (Carlsbad, CA) ; anti-CDKN1A clone SXM30 (#556431) from BD Pharmingen; anti-IκBα (C-21, sc-371), anti-MCL1 (S-19, sc-819), anti-CBP (F-12, sc-365915), anti-p300 (C-20, sc-585) and anti-IL-21R (L-20, sc-23075) from Santa Cruz Biotechnologies (Dallas, TX); anti-TCL1A clone 27D6/20 (#K0028-3) from Medical & Biological Laboratories Co. (Woburn, MA); anti-cMyc (Y69, ab32072) from Abcam (Cambridge, MA); and anti-GAPDH (#MAB374) from Millipore (Billerica, MA). Anti-BRD4 (#A301-985A-M) from Bethyl Laboratories was used to detect mouse BRD4. Species-appropriate secondary antibodies were obtained from Bio-Rad (Hercules, CA). After antibody incubations, proteins were detected with chemiluminescent substrate (WesternBright, Advansta Inc, Menlo Park, CA).

Antibodies used for ChIP included anti-H3K27ac (#39133) and anti-RNA Pol II (#39097) from Active Motif; and anti-BRD4 (#A301-985A100) from Bethyl Laboratories (Montgomery, TX).

For qPCR analysis the following TaqMan® gene expression assays were purchased from Life Technologies: BRD4 (ID: Hs04188085_m1), SYK (ID: Hs00895377_m1), BTK (ID: Hs00975865_m1), BLK (ID: Hs01017458_m1) , PIK3CG (ID: Hs00277090_m1), ZAP70 (ID: Hs00896345_m1), TCL1A (ID: Hs00951350_m1), CDKN1A (ID: Hs00355782_m1), HEXIM1 (ID: Hs00538918_s1), ZBTB17 (ID: Hs01114794_g1), MYC (ID: Hs00153408_m1), CXCR4 (ID: Hs00607978_s1), IL10RA (ID: Hs00155485_m1), BCL-XL (ID: Hs00236329_m1), BID (ID: Hs01026792_m1), PUMA (ID: Hs00248075_m1), BIM (ID: Hs00708019_s1), TBP (ID: Hs00427620_m1) and Human GAPDH Endogenous Control (# 4352934E). The PrimeTime®

Predesigned qPCR assays for IKZF1 (ID: Hs.PT.58.15361669) and IKZF3 (ID: Hs.PT.58.40618863) were purchased from Integrated DNA Technologies (Coralville, IA).

Quantitative PCR analysis of mouse splenocyte samples was performed using : a) the Fast SYBR™ Green Master Mix (Applied Biosystems) for the following primers *Mus musculus endogenous Myc* (F: CAG CTC CTC CTC GAG TTA G R: TGA GGA AAC GAC GAG AAC AG), *Mus musculus transgenic PhiX Myc* (F: TCG AAC AGC TTC GAA ACT CTG GTG R: TTA AAT CGA AGT GGA CTG CTG GCG) and *Mus musculus Gapdh* (F: CCT TCA TTG ACC TCA ACT AC R: GGA AGG CCA TGC CAG TGA GC) as murine control purchased from Integrated DNA Technologies; b) TaqMan™ Fast Advanced Master Mix (Applied Biosystems) for the following TaqMan® gene expression assays; TCL1A (ID: Hs00951350_m1), Tcl1 (ID: Mm00493475_m1), Hexim (ID: Mm01248328_s1), Myc (ID: Mm00487804_m1) and Tbp (ID: Mm00446973_m1) purchased from Life Technologies.

Animal studies: Disease progression was measured weekly by flow cytometric evaluation of % CD19/CD5/CD45 positive circulating cells (CD5-FITC, CD19-PE and CD45-APC (BD Pharmingen) and/or blood smears for total WBC counts.

Microarray analysis

Gene expression levels were summarized by RMA method(1). A filtering method based on percentage of arrays above noise cutoff was applied to filter out low expression genes. Linear model was employed to detect differentially expressed genes. In order to improve the estimates of variability and statistical tests for differential expression, a variance smoothing method with fully moderated t-statistic was employed for this study(2). The significance level was adjusted by controlling the mean number of false positives(3). Principle component analysis (PCA) was used to discriminate samples based on gene expression profiling(4). The data of all genes were projected onto multiple dimensions (i.e., PC1, PC2, and PC3) for each sample, where PC1, PC2, and PC3 are the first three dimensions with the largest variation of the expression data and they are the linear combinations of all genes' expression. Statistical software SAS 9.4 and R was used for analysis.

Histology and immunohistochemistry

Formalin-fixed spleens, lungs, hearts, and lymph nodes from study mice were paraffin-embedded, sectioned onto glass slides at 4 μM, then deparaffinated, hydrated with distilled water, and stained with hematoxylin and eosin (HE). For Ki67 staining, following hydration, sections were treated with citrate buffer pH 6.0 at 125°C for 15 min. 3 % hydrogen peroxide with methanol was used to block endogenous peroxidase. A serum-free protein block was applied, incubated for 10 min and rinsed. Staining was performed by sequential application and incubation with anti-Ki67 primary antibody (Thermo Scientific, Waltham, MA) using 1:100 dilution at room temperature, biotinylated goat anti-rabbit secondary antibody (Vector Labs, Burlingame, CA,

USA) for 30 min at room temperature, ABC biotinylated antibody linker (Vector Labs) for 30 min at room temperature, and DAB substrate (Dako, Carpinteria, CA) for 5 min. Hematoxylin was used as a counter stain.

ChIP-Seq and Data Processing: Genomic DNA (Input) was prepared by treating aliquots of chromatin with RNase, proteinase K and heat for de-crosslinking, followed by ethanol precipitation. Pellets were resuspended and the resulting DNA was quantified on a NanoDrop spectrophotometer. Extrapolation to the original chromatin volume allowed quantitation of the total chromatin yield. An aliquot of chromatin (30 ug) was precleared with protein A (G) agarose beads (Invitrogen). Sequence read data of a BRD4 ChIP-seq experiment for P493-6 cells (immortalized human peripheral B cells) were downloaded from GEO (sample GSM1036401 from series GSE42262)(5). The 75-nt single end sequence reads were mapped to the human reference genome (GRCh37/hg19) using the BWA algorithm (6) with default settings. Duplicate reads were removed and only uniquely mapped reads were used for further analysis. Alignments were extended in silico at their 3'-ends to a length of 200 bp, which is the average genomic fragment length in the size-selected library, and assigned to 32-nt bins along the genome. The resulting histograms of fragment densities were stored in bigWig files. Peak locations (enriched regions) for BRD4 and H3K27ac were determined using the MACS algorithm (7) (v1.4.2) with a cutoff p-value of $1E^{-7}$ for narrow peaks and $1E^{-1}$ for broad peaks. RNA Pol II-enriched regions were identified using the SICER algorithm (8) with a cutoff FDR of $1E^{-10}$ and gap parameter of 600bp. Super-enhancers were identified with ROSE software (9). First H3K27ac peaks within 12.5 kb of each other were stitched together to determine enhancer regions, and then top scoring ones are identified as super-enhancers. To compare the peak metrics between multiple samples, the peak intervals from all samples were merged, and aligned reads for these newly defined regions was extracted from bigWig files for all samples (even for those where no peak was called) using a custom Perl script (by ActiveMotif). The resulting matrix (rows = merged peak locations, columns = samples) was annotated with gene information by calculating distances from RefSeq gene starts and ends to the center of the merged peak regions, and applying an annotation cutoff of 10kb.

ATAC-seq and data processing: In each experiment, 10^5 cells were washed once in 50 µl PBS, resuspended in 50 µl ATAC-seq lysis buffer (10 mM Tris-HCl pH 7.4, 10 mM NaCl, 3 mM MgCl2 and 0.1% IGEPAL CA-630) and centrifuged for 10 min at 4 °C. On centrifugation, the pellet was washed briefly in 50 µl MgCl2 buffer (10 mM Tris pH 8.0 and 5 mM MgCl2) before incubating in the transposase reaction mix (12.5 µl 2 × TD buffer, 2 µl transposase (Illumina) and 10.5 µl nuclease-free water) for 30 min at 37 °C. After DNA purification with the MinElute kit, 1 µl of the eluted DNA was used in a qPCR reaction to estimate the optimum number of amplification cycles. Library amplification was followed by SPRI size selection to exclude fragments larger than 1,200 bp. DNA concentration was measured with a Qubit fluorometer (Life Technologies). Library

amplification was performed using custom Nextera primers. The libraries were sequenced by the Biomedical Sequencing Facility at CeMM using the Illumina HiSeq3000/4000 platform and the 25-bp paired-end configuration. The 150-nt paired end sequence reads were mapped to the human reference genome (GRCh37/hg19) using the Bowtie2 algorithm with maximum fragment length of 1000 and no-mixed mode. After removal of duplicate reads, DNase2hotspots (10) software package (https://sourceforge.net/projects/dnase2hotspots) was used to identify hotspots (enriched regions) from ATAC-seq. Consensus hotspots from all the treatment condition for each patient were generated as the union of the overlapping hotspots using R GenomicRanges package (11), then annotated using R ChIPpeakAnno package (12).

Statistical analyses

Differences in cell viability and apoptosis between conditions of interest were assessed using mixed effects models. Appropriate transformations of the data (e.g., log transform) were applied when necessary before modeling in order to stabilize variances. BRD4 expression was compared between CLL and normal patients using a two-sample t-test assuming unequal variances. For the mouse models, survival curve estimates were calculated using the Kaplan-Meier method and differences in curves between treatments groups were assessed using the log-rank test. Differences in PBL at different time points were assessed using a mixed effects model, and a two sample t-test assuming unequal variances was used to compare spleen weight. Analyses were formed using SAS/STAT software, version 9.4 of the SAS System for Windows (SAS Institute Inc., Cary, NC).

Chemical structure and synthesis of PLX51107

PLX51107 was synthesized from commercially available 6-bromo-1H-pyrrolo[3,2-b]pyridine **1** as described in WO2014145051. 6-bromo-1H-pyrrolo[3,2-b]pyridine was reacted with 3,5-dimethyl-4-(4,4,5,5-tetramethyl-1,3,2-dioxaborolan-2-yl)isoxazole under Suzuki coupling conditions to provide compound **2.** Compound **2** was treated NIS in acetonitrile to provide compound **3**, which was then reacted with (1R)-1-(2-pyridyl)ethanol under Mitsunobu reaction conditions to give compound **4**. Compound **4** when reacted with methyl 4-(4,4,5,5-tetramethyl-1,3,2-dioxaborolan-2-yl)benzoate under Suzuki coupling conditions provided compound **5** which upon hydrolysis gave (S)-4-(6-(3,5-dimethylisoxazol-4-yl)-1-(1-(pyridin-2-yl)ethyl)-1H-pyrrolo[3,2-b]pyridin-3-yl)benzoic acid **PLX51107**.

Scheme 1

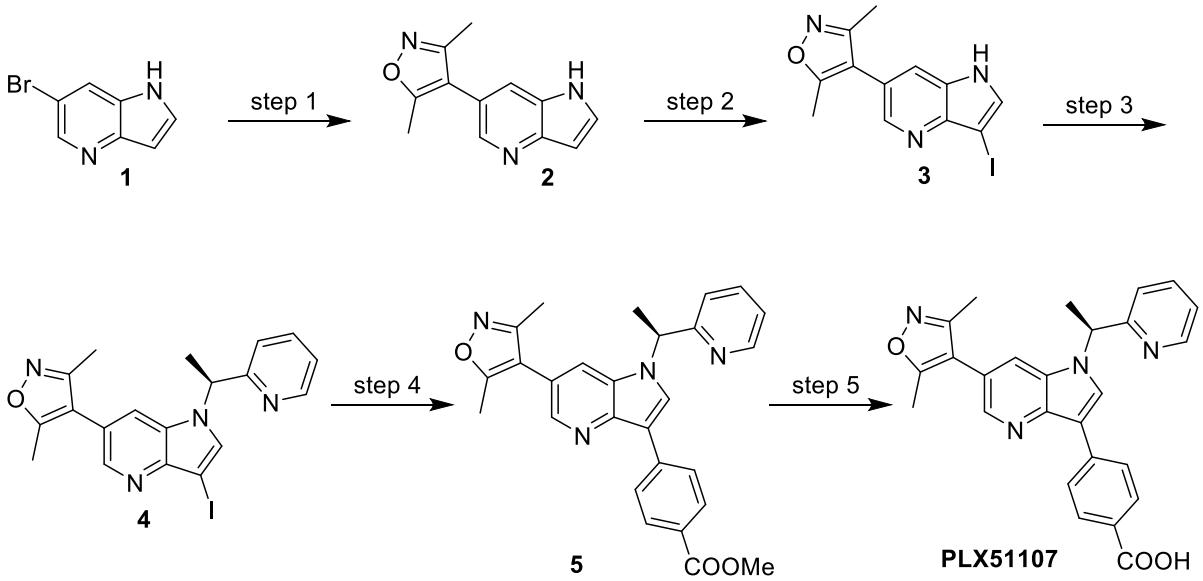

Step 1 – Preparation of 3,5-dimethyl-4-(1H-pyrrolo[3,2-b]pyridin-6-yl)isoxazole (2). To a high pressure bottle were added 6-bromo-1H-pyrrolo[3,2-b]pyridine (**1**, 2.5 g, 12.69 mmol), 3,5-dimethyl-4-(4,4,5,5-tetramethyl-1,3,2-dioxaborolan-2-yl)isoxazole (3.5 g, 15.69 mmol), [1,1'-bis(diphenylphosphino)ferrocene]dichloropalladium(II) (0.2 g, 0.26 mmol), 1M potassium carbonate in water (60 mL), and acetonitrile (120 mL). The reaction was heated at 160 °C overnight. The reaction was poured into water, and extracted with ethyl acetate. The organic layer was washed with brine, dried over sodium sulfate, and filtered. The filtrate was concentrated, and purified with silica gel column chromatography eluting with 20% to 100% ethyl acetate in hexane to give product (**2**, 1.95 g, 72.1%). ^{1}H NMR (400 MHz, DMSO-d_6): δ 11.39 (s, 1H), 8.28 (d, J = 1.6 Hz, 1H), 7.74 (s, 1H), 7.69-7.67 (m, 1H), 6.58 (s, 1H), 2.40 (s, 3H), 2.22 (s, 3H); MS (ESI) $[M+H^+]^+$ = 213.7.

Step 2 – Preparation of 4-(3-iodo-1H-pyrrolo[3,2-b]pyridin-6-yl)-3,5-dimethyl-isoxazole (3). To 3,5-dimethyl-4-(1H-pyrrolo[3,2-b]pyridin-6-yl)isoxazole (**2**, 1.7 g, 7.97 mmol) in acetonitrile (110 mL) and DMF (5 mL) was N-iodosuccinimide (1.88 g, 8.37 mmol) at room temperature. The reaction was stirred at room temperature for 4 hours. The reaction was poured into aqueous potassium carbonate, and extracted with ethyl acetate. The organic layer was washed with brine, dried over sodium sulfate, and filtered. The filtrate was concentrated, and purified with silica gel column chromatography eluting with 20% to 100% ethyl acetate in hexane to give product (**3**, 2.6 g, 96.2%). ^{1}H NMR (400 MHz, DMSO-d_6): δ 11.84 (s, 1H), 8.36 (d, J = 1.6 Hz, 1H), 7.88 (d, J = 2.8 Hz, 1H), 7.77 (d, J = 2.0 Hz, 1H), 2.41 (s, 3H), 2.22 (s, 3H); MS (ESI) $[M-H^+]^-$ = 338.0.

Step 3 – Preparation of 4-[3-iodo-1-[(1S)-1-(2-pyridyl)ethyl]pyrrolo[3,2-b]pyridin-6-yl]-3,5-dimethyl-isoxazole 4. To 4-(3-iodo-1H-pyrrolo[3,2-b]pyridin-6-yl)-3,5-dimethyl-isoxazole (**3**, 0.92 g, 2.71 mmol) in THF (20 mL) were added (1R)-1-(2-pyridyl)ethanol (0.38 g, 3.09 mmol), and

triphenylphosphine (0.96 g, 3.65 mmol). The reaction was cooled with ice water, followed by adding diisopropyl azodicarboxylate (0.47 mL, 2.38 mmol) dropwise for about 15 minutes. After 1 hour, the reaction was allowed to warm to room temperature for 1 hour. The reaction was concentrated, and purified with silica gel column chromatography eluting with 20% to 100% ethyl acetate in hexane to give product (**4**, 0.91 g, 75.5%). ^{1}H NMR (400 MHz, DMSO-d_6): δ 8.51-8.50 (m, 1H), 8.36 (d, *J* = 2.0 Hz, 1H), 8.18 (s, 1H), 7.92 (d, *J* = 1.6 Hz, 1H), 7.75 (dt, *J* = 1.6, 8.0 Hz, 1 H), 7.37 (d, *J* = 8.0 Hz, 1H), 7.29-7.26 (m, 1H), 6.01 (q, *J* = 7.2 Hz, 1H), 2.35 (s, 3H), 2.17 (s, 3H), 1.92 (d, *J* = 7.2 Hz, 3H); MS (ESI) $[M+H^+]^+$ = 445.0.

Step 4 – Preparation of methyl 4-[6-(3,5-dimethylisoxazol-4-yl)-1-[(1S)-1-(2-pyridyl)ethyl]pyrrolo[3,2-b]pyridin-3-yl]benzoate 5. To 4-[3-iodo-1-[(1S)-1-(2-pyridyl)ethyl]pyrrolo[3,2-b]pyridin-6-yl]-3,5-dimethyl-isoxazole (**4**, 0.5 g, 1.13 mmol) in THF (16 mL) were added methyl 4-(4,4,5,5-tetramethyl-1,3,2-dioxaborolan-2-yl)benzoate (0.38 g, 1.46 mmol), [1,1'-bis(diphenylphosphino)ferrocene]dichloropalladium(II) (0.05 g, 0.07 mmol), and 1M *potassium* carbonate in water (8 mL). The reaction was stirred for 2 hours at 70 ^{o}C, then poured into water, and extracted with ethyl acetate. The organic layer was washed with brine, dried over sodium sulfate, and filtered. The filtrate was concentrated, and purified with silica gel column chromatography eluting with 20% to 100% ethyl acetate in hexane to give product (**5**, 0.37 g, 72.7%). ^{1}H NMR (400 MHz, DMSO-d_6): δ 8.73 (s, 1H), 8.52-8.48 (m, 4H), 8.00-7.99 (m, 3H), 7.77-7.73 (m, 1H), 7.39 (d, *J* = 7.6 Hz, 1H), 7.28-7.25 (m, 1H), 3.64 (s, 3H), 2.38 (s, 3H), 2.19 (s, 3H), 2.00 (d, *J* = 7.2 Hz, 3H); MS (ESI) $[M+H^+]^+$ = 453.3.

Step 5- preparation of (S)-4-(6-(3,5-dimethylisoxazol-4-yl)-1-(1-(pyridin-2-yl)ethyl)-1H-pyrrolo[3,2-b]pyridin-3-yl)benzoic acid PLX51107. To methyl 4-[6-(3,5-dimethylisoxazol-4-yl)-1-[(1S)-1-(2-pyridyl)ethyl]pyrrolo[3,2-b]pyridin-3-yl]benzoate (**5**, 0.32 g, 0.71 mmol) in THF (6.0 mL) was added 2M lithium hydroxide (3 mL). The reaction mixture was stirred at 60 °C overnight. The reaction was poured into water, acidified to pH around 6 with 1N of HCl (6 mL), extracted with ethyl acetate. The organic layer was washed with brine, and the organic layer was dried over sodium sulfate, concentrated, and washed with ethyl acetate and hexane to give product (**PLX51107**, 261.1 mg, 84.2%). ^{1}H NMR (400 MHz, DMSO-d_6): δ 12.75 (s, 1H), 8.70 (s, 1H), 8.52-8.47 (m, 4H), 8.00-7.95 (m, 3H), 7.77-7.73 (m, 1H), 7.39 (d, *J* = 7.6 Hz, 1H), 7.28-7.25 (m, 1H), 6.06 (q, *J* = 7.2 Hz, 1H), 2.38 (s, 3H), 2.19 (s, 3H), 2.00 (d, *J* = 7.2 Hz, 3H); MS (ESI) $[M+H^+]^+$ = 438.9.

Crystallization and Structure determination

To enable crystallization, human BRD4 fragment encoding the N-terminal bromodomain (BD1, residues N44-E168) was expressed in *Escherichia coli* cells following published procedure(13).

Co-crystallization of BRD4-BD1 and PLX5981 was carried out using the sitting drop vapor diffusion method. 1 µL protein-ligand solution (with a final concentration of 10mg/mL protein and 1mM ligand, respectively) was mixed with 2 µL reservoir solution (0.1 M Bis-Tris Propane; pH7.5-8.0, 11 % PEG3350, 0.2 M NaCl and 20 % Ethylene glycol) in the drop and allowed to equilibrate against the reservoir at 4°C. Crystals grew to full size within 6-8 days and were harvested and flash-frozen with liquid nitrogen. Similar setup with PLX51107 did not yield any crystal. Analysis of crystal packing and modeling the binding of PLX51107 suggested that the side chain of Asp96 from a neighboring BRD4 molecule may preclude compound access to ZA channel. Hence co-crystallization experiments were performed using D96A mutant protein ($BRD4^{D96A}$) wherein 2 µL protein-ligand solution and 2 µL reservoir solution (0.1 M Bis-Tris; pH7.5, 19 % PEG3350, 0.2 M Li-Sulfate) were set up in each drop. For cryoprotection, co-crystals of BRD4-BD1 with PLX51107 or OTX015 were soaked into the reservoir supplemented with 15 % glycerol prior to freezing. X-ray diffraction data were collected at synchrotrons ALS8.3.1 (Lawrence Berkeley National Laboratory, Berkeley CA) and SSRL7.1 (Stanford University, Stanford, CA). These datasets were processed and scaled using MOSFLM(14) and SCALA(15) in the CCP4 package(16) (**Table S3**). Structures were solved by the molecular replacement method with the program MOLREP(17) using a published structure (PDB ID: 2OSS) as a searching model. The initial model was subjected to rigid body and restrained refinement using the program PHENIX(18). Riding hydrogen atoms (only for datasets of $BRD4^{D96A}$-PLX51107 and $BRD4^{D96A}$-OTX015) and water molecules were added; and the weights for the X-ray/stereochemistry and X-ray/ADP were optimized to achieve the lowest R_{free} value. B-factors of the atoms were refined anisotropically for all non-hydrogen atoms. Electron density for compound was clearly visible and was then modeled in at this stage to avoid model bias. COOT(19) was used to manually rebuild and monitor the structure, followed by refinement until no further improvement in R_{free}.

Binding assay and selectivity profiling

Binding interactions of PLX51107 to a panel of 32 isolated bromodomains were measured using BROMOscan (DiscoveRx, Fremont, CA) (**Table S1**). A test compound that binds the bromodomain active site and prevents bromodomain binding to the immobilized ligand reduces the amount of protein captured on the solid support. The amount of bromodomain captured was quantified by a precise and ultra-sensitive qPCR method that detects the associated DNA label. In the single concentration primary screen, screening "hits" were identified by measuring the amount of bromodomain captured in test versus control samples and the results were reported as %inhibition. In a similar manner, the dissociation constant (K_d) for test compound-bromodomain interactions was calculated by measuring the amount of bromodomain protein captured on the solid support as a function of the test compound concentration. BROMOscan assays use trace bromodomain concentrations and thereby report true thermodynamic inhibitor K_d values over a broad range of affinities (<0.1 nM to >10 µM).

Time-resolved fluorescence resonance energy transfer (TR-FRET) assay to determine compound offrates

Reagent: ST-BRD4-BD12 (BPS #31044, San Diego, CA), Strep-Alexa Fluor 647 (Life Technologies, S-32357, Chicago, IL), LanthaScreen Europium-labeled (Eu) anti-GST antibody (Life Technologies #PV5594, Chicago, IL), 3X BRD TR-FRET assay buffer 1(BPS #33012, San Diego, CA), H4K5/8/12/16 (Ac)-Biotin (Anaspec #64989, Fremont, CA).

PLX51107, OTX-015 (both at 1.5 μM) or DMSO vehicle control was incubated with GST-BRD4 (truncated protein containing both BD1 and BD2) (300nM) and Eu-anti-GST (300nM) in 1xTR-FRET buffer for 1 hour. Tracer was prepared by incubating 12.5 nM Strep-Alexa 647 with 50 nM H4K5/8/12/16(Ac)-biotin peptide in 1xTR-FRET buffer for 1 hour. 2 μL of BRD4/inhibitor mixture was then diluted into 198 uL of prepared tracer. Following dilution, the samples were read continuously to monitor the change in TR-FRET signal over time. Binding of the tracer and Eu labeled antibody to BRD4 results in FRET signal, whereas displacement of the tracer with a BRD4 inhibitor results in a loss of FRET. As the inhibitor dissociates and the tracer binds, the TR-FRE signal increases. The raw data are converted into percent of control signal (DMSO 100% and no BRD4 protein 0%).

GenScript cell panel

The antitumor effects of PLX51107 were evaluated in a broader panel of 69 hematopoietic cell lines (38 leukemia cell lines and 31 lymphoma cell lines) at GenScript (Piscataway, NJ). These cell lines harbor a range of genetic aberrations observed in patients with lymphomas and leukemias. PLX51107 was assayed at seven 3-fold dilutions in duplicate beginning at 20 μM with a CellTiter-Glo luminescent Cell Viability Assay that measures cellular ATP content. Dose response of doxorubicin on BEL-7402 cells was included in each plate as an internal control.

Pharmacokinetics in mice, rats and dogs

To determine the pharmacokinetics of PLX51107 in mice, rats and dogs over 24 h, PLX51107 was administered as a single dose intravenously (i.v.) to groups of three male CD-1 mice (at 1 mg/kg dose), three male Sprague–Dawley rats (at 1 mg/kg dose) or three Beagle dogs of mixed genders (at 0.5 mg/kg dose). For i.v. dosing, PLX51107 DMSO solution was mixed with a vehicle that consisted of 10% (w/w) solutol, 10% (w/w) ethanol and 80% (w/w) water (dosing volume 5 mL/kg in mice and rats and 1 mL/kg in dogs). Two hundred microliters (mice) or 250 μL (rats) of whole blood was collected via inferior vena cava (mice) or jugular vein cannula (rats) or leg (dogs) before compound administration and at the following time points: 0.25, 0.5, 1, 2, 4, 8, and 24 h for mice and rats and 0.5, 1, 2, 3, 4, 6, 8 and 24 h for dogs.

Mouse splenomegaly model

The inhibitory activities of BET inhibitors on B-cell malignancies were compared in a Ba/F3 splenomegaly model. The murine bone marrow-derived pro-B-cell line, Ba/F3, depends on the addition of IL-3 for growth in cell culture. However Ba/F3 cells engineered to express an oncogene are capable of factor-independent growth, but become apoptotic when the oncogene or its downstream signaling is inhibited in this model(20). When injected into the tail veins of nude mice, the factor-independent Ba/F3 cells home to the spleen and proliferate, leading to a marked splenomegaly. The *in vivo* proliferation of the factor-independent Ba/F3 cells and appearance of splenomegaly can be blocked by oral administration of BET inhibitors. Five different doses of PLX51107 (0.5, 1, 2, 5, and 10 mg/kg) and OTX015 (5, 10, 25, 50, and 100 mg/kg) and vehicle control were administered orally to mice 6 days after Ba/F3-engraftment and the dosing continued for 7 days before PK analysis and spleen weight measurement.

MV4-11 xenograft model, RNA-seq and PK analysis

Eight SCID mice with MV4-11 xenografts were used to measure the gene expression kinetics of a single 20 mg/kg dose of PLX51107. Six mice were dosed with the compound and two mice were taken down at each time point (0 hours, 2 hours, 4 hours and 8 hours post-dose). Fresh tumor pieces (< 100 mg) were stabilized with RNAlater. RNA was isolated with Qiagen RNeasy columns according to the manufacturer's protocol. RNA quality was assessed with the fragment analyzer and quantified with the nanodrop. 1000 ng of RNA were used to prepare a sequencing library for each sample using a Stranded RNA-seq kit with Ribo-Erase (KAPA Biosystems). Libraries were sequenced on a HiSeq4000 generating 100 bp reads. Reads were trimmed with trimmomatic prior to separation of human from mouse reads with xenomatic. Human reads were aligned with STAR aligner and then transcript counts were generated with the featureCounts function from the Rsubread package. Reads per kilobase of transcript per million mapped reads (rpkm) were calculated with the rpkm function from the edgeR package. This work used the Vincent J. Coates Genomics Sequencing Laboratory at UC Berkeley, supported by NIH S10 OD018174 Instrumentation Grant.

In a satellite PK study, four SCID mice with MV4-11 xenografts were given a single dose of 20 mg/kg PLX51107. Blood was collected at 0.5, 1, 2, 4 and 8 hours after dosing for pharmacokinetic analysis. All PK parameters were calculated using Phoenix 7.0 (Certara, Princeton, NJ).

References

1. Irizarry RA, Hobbs B, Collin F, Beazer-Barclay YD, Antonellis KJ, Scherf U*, et al.* Exploration, normalization, and summaries of high density oligonucleotide array probe level data. Biostatistics **2003**;4(2):249-64 doi 10.1093/biostatistics/4.2.249.

2. Yu L, Gulati P, Fernandez S, Pennell M, Kirschner L, Jarjoura D. Fully moderated T-statistic for small sample size gene expression arrays. Statistical applications in genetics and molecular biology. Volume 102011. p 1631-6.
3. Gordon A, Glazko G, Qiu X, Yakovlev A. Control of the mean number of false discoveries, Bonferroni and stability of multiple testing. **2007**:179-90 doi 10.1214/07-AOAS102.
4. DW. JRaW. Applied Multivariate Statistical Analysis. 5th edition. . Fourth Edition, Prentice Hall, New Jersey, 07458 **1998**.
5. Lin CY, Loven J, Rahl PB, Paranal RM, Burge CB, Bradner JE*, et al.* Transcriptional amplification in tumor cells with elevated c-Myc. Cell **2012**;151(1):56-67 doi 10.1016/j.cell.2012.08.026.
6. Li H, Durbin R. Fast and accurate short read alignment with Burrows-Wheeler transform. Bioinformatics **2009**;25(14):1754-60 doi 10.1093/bioinformatics/btp324.
7. Zhang Y, Liu T, Meyer CA, Eeckhoute J, Johnson DS, Bernstein BE*, et al.* Model-based Analysis of ChIP-Seq (MACS). Genome biology **2008**;9(9):R137 doi 10.1186/gb-2008-9-9-r137.
8. Zang C, Schones DE, Zeng C, Cui K, Zhao K, Peng W. A clustering approach for identification of enriched domains from histone modification ChIP-Seq data. Bioinformatics **2009**;25(15):1952-8 doi 10.1093/bioinformatics/btp340.
9. Whyte WA, Orlando DA, Hnisz D, Abraham BJ, Lin CY, Kagey MH*, et al.* Master transcription factors and mediator establish super-enhancers at key cell identity genes. Cell **2013**;153(2):307-19 doi 10.1016/j.cell.2013.03.035.
10. Baek S, Sung MH, Hager GL. Quantitative analysis of genome-wide chromatin remodeling. Methods in molecular biology **2012**;833:433-41 doi 10.1007/978-1-61779-477-3_26.
11. Lawrence M, Huber W, Pages H, Aboyoun P, Carlson M, Gentleman R*, et al.* Software for computing and annotating genomic ranges. PLoS computational biology **2013**;9(8):e1003118 doi 10.1371/journal.pcbi.1003118.
12. Zhu LJ, Gazin C, Lawson ND, Pages H, Lin SM, Lapointe DS*, et al.* ChIPpeakAnno: a Bioconductor package to annotate ChIP-seq and ChIP-chip data. BMC bioinformatics **2010**;11:237 doi 10.1186/1471-2105-11-237.
13. Filippakopoulos P, Qi J, Picaud S, Shen Y, Smith WB, Fedorov O*, et al.* Selective inhibition of BET bromodomains. Nature **2010**;468(7327):1067-73 doi 10.1038/nature09504.
14. Andrew G. W. Leslie, Powell HR. Processing diffraction data with mosflm. Evolving Methods for Macromolecular

Crystallography. Volume 245, NATO Science Series. P.O. Box 17, 3300 AA Dordrecht, The Netherlands.: Springer; 2007. p 41-51.

15. Evans P. Scaling and assessment of data quality. Acta crystallographica Section D, Biological crystallography **2006**;62(Pt 1):72-82 doi 10.1107/s0907444905036693.
16. The CCP4 suite: programs for protein crystallography. Acta crystallographica Section D, Biological crystallography **1994**;50(Pt 5):760-3 doi 10.1107/s0907444994003112.
17. Vagin A, Teplyakov A. MOLREP: an Automated Program for Molecular Replacement. Journal of Applied Crystallography **1997**;30(6):1022-5 doi doi:10.1107/S0021889897006766.
18. Adams PD, Afonine PV, Bunkoczi G, Chen VB, Davis IW, Echols N*, et al.* PHENIX: a comprehensive Python-based system for macromolecular structure solution. Acta crystallographica Section D, Biological crystallography **2010**;66(Pt 2):213-21 doi 10.1107/s0907444909052925.
19. Emsley P, Cowtan K. Coot: model-building tools for molecular graphics. Acta crystallographica Section D, Biological crystallography **2004**;60(Pt 12 Pt 1):2126-32 doi 10.1107/s0907444904019158.
20. Mercher T, Wernig G, Moore SA, Levine RL, Gu TL, Frohling S*, et al.* JAK2T875N is a novel activating mutation that results in myeloproliferative disease with features of megakaryoblastic leukemia in a murine bone marrow transplantation model. Blood **2006**;108(8):2770-9 doi 10.1182/blood-2006-04-014712.